IOPscience iopscience.iop.org

Home Search Collections Journals About Contact us My IOPscience

Dielectric relaxation and defect analysis of Ta_2O_5 thin films

This content has been downloaded from IOPscience. Please scroll down to see the full text.

2000 J. Phys. D: Appl. Phys. 33 1137

(http://iopscience.iop.org/0022-3727/33/10/301)

View the table of contents for this issue, or go to the journal homepage for more

Download details:

IP Address: 140.113.38.11
This content was downloaded on 28/04/2014 at 07:56

Please note that terms and conditions apply.

J. Phys. D: Appl. Phys. **33** (2000) 1137–1142. Printed in the UK PII: S0022-3727(00)08425-4

Dielectric relaxation and defect analysis of Ta_2O_5 thin films

S Ezhilvalavan†, Ming Shiahn Tsai and Tseung Yuen Tseng‡

Department of Electronics Engineering and Institute of Electronics, National Chiao-Tung University, Hsinchu-300, Taiwan, Republic of China

E-mail: tseng@cc.nctu.edu.tw

Received 5 October 1999, in final form 22 February 2000

Abstract. The presence of defects in thin-film dielectrics often leads to dielectric relaxation as a function of frequency, in which the dielectric constant decreases and the loss tangent increases with increasing frequency. Dielectric relaxation results in charge storage capacity reduction under dynamic random access memory operating conditions. In this work, the dielectric relaxation behaviour of dc reactive sputtered Ta_2O_5 thin film was investigated. Using dielectric dispersion measurements as a function of frequency ($100\ \mathrm{Hz} \leqslant f \leqslant 10\ \mathrm{MHz}$) and temperature ($27\,^{\circ}\mathrm{C} \leqslant T \leqslant 150\,^{\circ}\mathrm{C}$), we determined the dielectric relaxation and defect quantity of the films and propose an equivalent circuit on the basis of complex capacitance, admittance and impedance spectral studies.

1. Introduction

In recent years, there has been an increasing interest in tantalum pentoxide (Ta_2O_5) thin films for high-density dynamic random access memory (DRAM) applications [1–4]. However, before Ta_2O_5 can be successfully utilized for device integration its material properties need to be better understood. The important electrical properties of Ta_2O_5 thin films that impact DRAM performance are its charge storage capacity, dissipation of stored charge or leakage current density and reliability [4–6].

In the previous studies, we reported that a short-duration rapid thermal annealing in O_2 at 800 °C was effective in improving the electrical properties of Ta_2O_5 capacitor films with a metal–insulator–metal (MIM) structure [7, 8]. Ta_2O_5 films with Pt electrodes exhibit high capacitance and low leakage current densities [7, 9]. However, high dielectric dispersion, i.e. frequency-dependent loss in capacitance is a challenging problem in the development of Ta_2O_5 capacitors for DRAM. It has been shown that dielectric relaxation phenomena in thin-film capacitors greatly affect their electrical properties [10–12]. Dielectric relaxation arises due to the dispersive nature of dielectric and increases with increasing value of the power law dependence of capacitance on frequency, which is termed as the dispersion parameter [13].

The most crucial influence of the dielectric relaxation on DRAM operation is that on the pause refresh property [14]. Horikawa *et al* [15] estimated that charge loss by the dielectric relaxation for the pause time of 1 s would amount to about 8% of the initially stored charge, which is about two orders of magnitude larger than that by its dc leakage current. Therefore, it is important to investigate the origin of the dielectric relaxation and its reduction.

Complex-plane analysis has proven to be a useful means of characterizing the electrical nature of a number of electroceramic materials [12, 16, 17]. In this analytical technique, measured sample ac data are examined in three complex-plane loci (capacitance, impedance and admittance). A semicircular fit of the data in any of these planes suggests an appropriate equivalent circuit representation of the observed dispersion. This approach can reveal the presence of relaxation processes and the relative contribution of defect states to the total ac response under a given set of experimental conditions. Recently several works were carried out using this technique in thin-film capacitors to explain the nature of dielectric relaxation [12, 18, 19]. However, to our knowledge, detailed studies on the dielectric relaxation and defect quantity analysis of dc reactively sputtered Ta_2O_5 thin films have not been reported so far. The purpose of the present study is to describe the nature and origin of dielectric relaxation for Ta_2O_5 thin films in a wide range of frequencies and to use the results to examine the suitability of the films for DRAMs. This paper also reports the observed shallow defect states and estimated defect densities of interface and grain boundary defects using admittance spectroscopy, which helps in a better understanding of the influence of the dielectric relaxation on the electrical properties of Ta_2O_5 films.

2. Background

There are at least four possible defects, namely the interface defect, grain boundary defect, shallow trap levels and oxygen vacancies, which may exist in MIM capacitor films, and

† Present address: 21 Physics and Astronomy, Michigan State University, East Lansing, MI-48824-1116, USA.
‡ Author to whom correspondence should be addressed.

 © 2000 IOP Publishing Ltd

which lead to dielectric relaxation as a function of frequency [12, 16, 20]. In the case of grain boundary defects, it is considered that the grain boundary in dielectric ceramics represents a resistor R and the grain is a thin insulating layer, C. There are many such RC series equivalent circuits in parallel throughout the ceramic. The equivalent circuit analysis by various researchers [12, 16–18] indicates that the grain boundary plays a prominent role in the relaxation of ceramics. The grain boundary defect exists within the non-stoichiometric grain boundary and the dominant defect is the oxygen vacancy. In the case of interface defect, it exists within the forbidden gap due to the interruption of the periodic lattice structure. Under the dc electric field the migration of oxygen vacancies followed by a reduction reaction leads to space charge accumulation at the grain boundary and the interface of the dielectric/electrode, reduces the barrier height at the grain boundary and interfaces increases the leakage current and exhibits the dielectric relaxation [12, 20]. The current induced by grain boundary defects is attributed to Poole–Frenkel conduction and the current induced by the interface defect is termed a Schottky emission [9].

The grain boundary defects and interface defects can be also determined by dc measurement under stress [12]. The shallow traps can be determined under small-signal ac stress applied at various temperatures. Under small-signal ac stress applied at the Schottky junction, the depletion layer width varies about its equilibrium position due to trapping and detrapping of electrons from the oxygen vacancies or shallow traps, denoted by E_t, where E_t is the trap energy. The shallow trap is located below, but near, the conduction band and hence its emission rate will be affected by temperature.

In addition to direct examination of the grain and/or grain boundary, complex-plane analysis is commonly adopted to separate and identify the inter/intragranular impedance and also to determine the contribution of defects on the dielectric relaxation. The electrical parameters used to characterize the ac response of a thin-film dielectric with parallel plane electrodes are impedance (Z) and admittance (Y). They have the following transformation relationships:

$$Y(\omega) = I(\omega)/V(\omega) = G_p(\omega) + \mathrm{j}B_p(\omega) \tag{1}$$

$$Z(\omega) = V(\omega)/I(\omega) = R_s(\omega) + \mathrm{j}X_s(\omega) \tag{2}$$

$$Y(\omega) = \mathrm{j}\omega \times C(\omega) = \mathrm{j}\omega \times (C' - \mathrm{j}C'') = \mathrm{j}\omega C_0 \times (\varepsilon' - \mathrm{j}\varepsilon''). \tag{3}$$

The following relations can be obtained by comparing equations (1)–(3):

$$G_p(\omega) = \omega C'' = \omega C_0 \varepsilon'' \tag{4}$$

$$B_p(\omega) = \omega C' = \omega C_0 \varepsilon' \tag{5}$$

where ω is the angular frequency, $I(\omega)$ and $V(\omega)$ are, respectively, the electrical current and applied voltage as functions of ω; $G_p(\omega)$ and $B_p(\omega)$ are, respectively, the parallel relative real admittance and imaginary admittance as functions of ω; $R_s(\omega)$ and $X_s(\omega)$ are, respectively, the series relative real impedance and imaginary impedance as functions of ω; C_0 is the geometric capacitance in free space; ε' and ε'' are the relative real and imaginary dielectric constant, respectively; and C' and C'' the real and imaginary capacitances, respectively.

Typically, results from impedance spectroscopy measurements are analysed via complex impedance and admittance plots, in which the imaginary part is plotted against the real part. The resulting curve is parameterized by the applied frequency, with low frequencies at a high real axis intercept and high frequencies at a low intercept. Depending on the distinctive orders of magnitude for the relaxation time, which is defined as the time-constant RC in the equivalent circuit to be an indication of the transport process, a series array of parallel RC elements may give rise to independent or overlapping semicircular arcs in the two complex planes. Complex impedance measurements are of great interest because they allow separation of the contributions of the grains, grain boundaries and defect states in the total impedance. The shape of the complex-plane plot is usually analysed using equivalent circuit analysis, where a collection of resistors and capacitors arranged in various combinations of series and parallel circuits are used to duplicate the experimental spectrum.

3. Experimental details

The deposition of Ta_2O_5 films in this study were performed on the Pt/SiO_2/n-Si substrate by dc-magnetron sputtering from a high-purity tantalum metal target (2.5 inch in diameter). The Ta_2O_5 film was prepared at a fixed power of 35 mW and at a constant pressure of 10 mTorr. The sputtering gas consists of a 80% Ar and 20% O_2 mixture with a total pressure of 10 mTorr. More details on the deposition technique may be found in [7, 9]. The film thickness was estimated to be 100 nm by using both ellipsometry with 632.8 nm wavelength He–Ne laser light source (Rudoph Research) and Tencor Alpha-step 200 profilometer. The rapid thermal annealing (RTA) of the Ta_2O_5 film was performed at 800 °C for 30 s in O_2 ambient, before patterning the top electrode in a RTA furnace (Ulvac Sinku-Rico, HPC 700). The RTA process temperature (800 °C) and annealing time (30 s) were chosen based on our earlier study [7, 9]. The heating rate used was the maximum heating rate of about 100 °C s^{-1}. The Pt top electrode with a thickness of 100 nm and diameters of 150, 250 and 350 μm were patterned by a shadow mask process. The current–voltage (I–V) characteristics of the Ta_2O_5 films were measured on the MIM structure with a delay time of 30 s using a HP4145B semiconductor parameter analyser. The capacitance–voltage (C–V) characteristic, admittance and impedance data were recorded at frequencies ranging from 100 Hz to 10 MHz with a 0.1 V ac sweeping signal using HP4194A impedance-gain phase analyser at various measurement temperatures (27–150 °C).

4. Results and discussion

Previous studies on the reactively sputtered Ta_2O_5 films indicated that a very-short-duration RTA process at 800 °C in O_2 for 30 s crystallized the films, decreased the leakage current density (10^{-10} A cm^{-2} at 100 kV cm^{-1}), increased the dielectric constant (52) and resulted in the best reliable time-dependent dielectric breakdown characteristics. More details

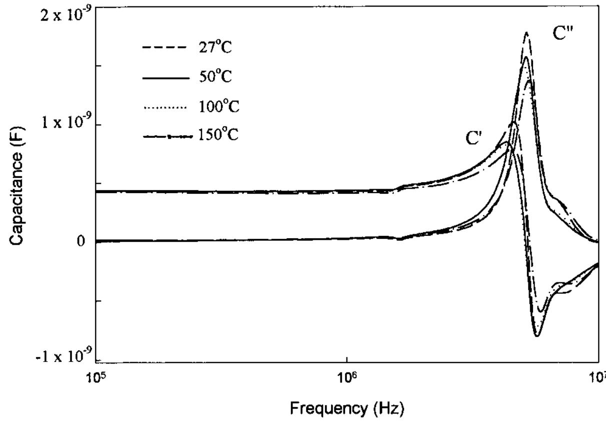

Figure 1. Frequency dependence of the relative real capacitance (C'), and imaginary capacitance (C'') of Ta_2O_5 thin films at various temperatures.

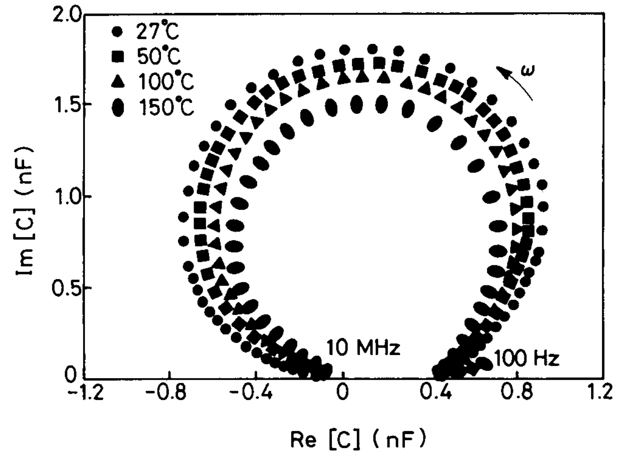

Figure 2. Complex capacitance plot of Ta_2O_5 thin films at various temperatures.

on the electrical and structural properties of the films were presented in our recent papers [7–9]. In the following sections the detailed complex capacitance analysis of Ta_2O_5 thin films in both high (>1 MHz) and low (<1 MHz) frequencies are presented.

4.1. High-frequency analysis (>1 MHz)

The frequency dependence of the real and imaginary capacitances for Ta_2O_5 thin films in the measurement temperature range of 27–150 °C is shown in figure 1. At high frequencies (>1 MHz), the capacitance increases, goes through a maximum and decreases abruptly, passing through zero and attains negative values, i.e. the Ta_2O_5 capacitor film shows a resonance in capacitance at high frequency between 1 and 10 MHz. Figure 2 shows the complex capacitance plot of Ta_2O_5 thin films measured at various temperatures. At high frequencies (1–10 MHz), the resonance phenomenon emerges as a circle in the complex capacitance plane (C^*). The complex capacitance plot in the high-frequency region continues to exhibit an abrupt discontinuity in dispersion with increasing frequency, which indicates the onset of a resonance phenomenon. The admittance ($G_p/\omega = C''$) at a given capacitance is constant over a narrow range of frequency on the complex capacitance curve in the C^* plane. Therefore the locus of the C'' is a circle of diameter $1/R_r$, tangential to the imaginary axis and with its centre displaced from the real axis in the positive direction. The lower the value of R_r, the higher will be the area of the circle [21].

At high frequencies, the films experience completely-shorted, grain boundary electrical barriers and become electrically conductive, resulting in negative capacitance and associated resonance in capacitance. A similar phenomenon was observed in polycrystalline ZnO varistors at frequencies >1 MHz [21, 22] and this effect was attributed to the type and density of defect states that are formed at the depletion regions of the grain boundary of the varistor ceramics [21, 22].

To understand the negative capacitance behaviour, it is first necessary to understand how the capacitance is measured. A harmonic voltage is impressed across the sample and the resulting harmonic current flow is measured. The general response of a charge-trapping grain boundary to an applied dc plus harmonic voltage of frequency ω, is given by

$$V(t) = V_{dc} + V_{ac}\sin\omega t \tag{6}$$

The current is generally of the form

$$J = J_{dc} + J_i \sin\omega t + J_q \cos\omega t \tag{7}$$

where subscripts i and q denote the in-phase and the quadrature currents, respectively. The capacitance per unit area is defined as $J_q/\omega V_{AC}$, where J_q is generally a function of ω, V_{DC} and T. In equilibrium, one component of the capacitance results from the displacement currents at the edge of the depletion regions of the grain boundary. It is this component which represents the stored charge, as is usually expected. As V_{DC} is increased, the thickness of the depletion layer grows and the capacitance decreases slightly. The anomalous capacitance results from the modulation of conduction current, J, crossing the grain boundary where,

$$J = J_{dc} + J_i(1-\delta)\sin\omega t + \delta J_q \cos\omega t. \tag{8}$$

Because there is a time constant τ governing the exchange of charge between the bulk and boundary, the charge in the boundary cannot achieve its equilibrium value corresponding to the instantaneous value of the applied voltage. This causes the barrier height ($\phi_b(t)$) to be slightly out of phase with $V(t)$, and since $J \propto \exp[-\phi_b(t)/k_B T]$, the current develops an out-of-phase (quadrature) component. It is this part of quadrature current, J_q, which yields the anomalous capacitance. Detailed calculations by Pike [22] show that when majority carriers alone are important in the barrier charge trapping, the anomalous capacitance always auguments the normal capacitance ($C > 0$). However, when minority carriers are also involved, it is possible to have the sign of the effect reversed ($C < 0$), and thus have the apparent capacitance become negative [21, 22]. The presence of such possible minority carriers (holes) in semiconductors were observed by Tomozane *et al* [23].

Furthermore, the frequency dependence of capacitance for Ta_2O_5 thin films in the high-frequency region (>1 MHz) may be attributed to two possible factors, namely the piezoelectric resonance or to the total inductance of the Ta_2O_5

capacitor itself. The resonance frequency for the thickness mode is determined by the electromechanical coupling factor and should be in the range of 1–10 MHz for dielectric films with a thickness of 0.5 μm [24]. Also, since the resonance frequency and the thickness of the film as not constant (which they should be for an ideal piezoelectric device) [16], the additional contribution from piezoelectric grain resonance is eliminated. Also, it is to be noted that since we have carried out the lead corrections before performing the experiments, the observed resonance in capacitance is not related to lead inductance. Therefore, the results obtained from figures 1 and 2, demonstrate that the observed resonance in capacitance at frequencies greater than 1 MHz is an electrical resonance resulting from the total inductance of the Ta_2O_5 capacitor film. These results are similar to that observed for $Ba(Sr)TiO_3$ thin films reported by Tsai and Tseng [12]. And hence the Ta_2O_5 film can be equally represented by an electrical equivalent circuit consisting of resistance, capacitance and inductance (*R–C–L*) connected in series, which can be used to duplicate the Ta_2O_5 capacitor film [25], where the capacitance of the equivalent circuit is mainly determined by the capacitance of the Ta_2O_5 film and the inductance of the equivalent circuit is determined by the bulk conductivity of the Ta_2O_5 capacitor film.

4.2. Low-frequency analysis (<1 MHz)

The complex capacitance spectral studies clearly demonstrate that the Ta_2O_5 thin films exhibit a resonance in capacitance at frequencies above 1 MHz. Therefore, the proposition of *R–C–L* series equivalent circuit is reasonable only for measurement frequencies $\geqslant$1 MHz. However, the situation is different if we try to further analyse the impedance spectra of Ta_2O_5 thin films at a measurement frequency in the range of 100 Hz–1 MHz. The impedance (Z) of the equivalent *R–C–L* circuit can be written as

$$Z(\omega) = R_{eq} + \mathrm{j}\omega L_{eq} + 1/\mathrm{j}\omega C_{eq}. \quad (9)$$

The inductance value (ωL_{eq}) is one to two orders smaller than the capacitance value ($1/\mathrm{j}\omega C_{eq}$), for the frequency range 100 Hz $\leqslant f \leqslant$ 1 MHz and can be neglected. Hence, we can simplify the equivalent *R–C–L* circuit consisting of only capacitors (C_{eq}) and resistors (R_{eq}). Figure 3 shows the complex impedance plot of Ta_2O_5 thin films measured at various temperatures. As shown in the figure, the real part of the complex impedance coincides at one point on the Re(Z). This plot is fairly similar to the complex impedance plot for the *R–C* series equivalent circuit described by Jonscher [25]. Figure 4 depicts the complex admittance plot of Ta_2O_5 thin films measured at various temperatures. The high-frequency data correspond to a well developed inclined circular arc passing through the origin of the y-plane. The experimental data do in fact lie on the circular arc centred at a point below the real axis; this corresponds to the appearance of the depression angle, $\theta \neq 0$ and indicates a Cole–Cole type of relaxation phenomenon [26]. The area of the semicircle is found to decrease with increasing measurement temperature. Therefore, on the basis of our complex impedance and admittance spectral analysis, the ac response of Ta_2O_5 capacitor films in the frequency range

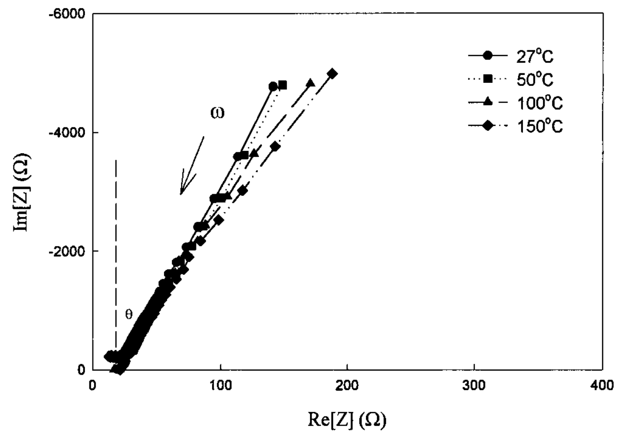

Figure 3. Complex impedance plot of Ta_2O_5 thin films at various temperatures for the frequency range of 100 Hz–1 MHz.

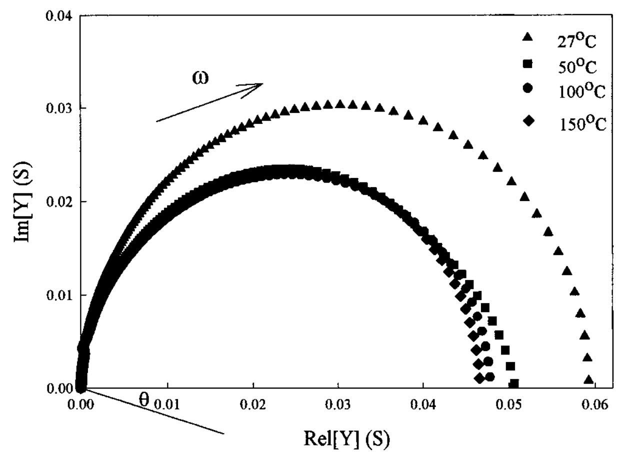

Figure 4. Complex admittance plot of Ta_2O_5 thin films at various temperatures for the frequency range of 100 Hz–1 MHz.

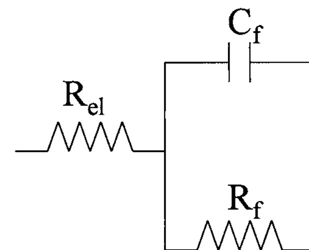

Figure 5. The schematic equivalent circuit model for Ta_2O_5 thin-film capacitors for the frequency range of 100 Hz–1 MHz.

of 100 Hz–1 MHz can be satisfactorily represented by a practical equivalent circuit as shown in figure 5. In the equivalent circuit, R_{el} represents the electrode resistance, C_f is the frequency-dependent capacitance due to the grain and R_f is the frequency-dependent resistance due to grain boundary and interface. The above equivalent circuit for a Ta_2O_5 capacitor film is similar to that for the $Ba(Sr)TiO_3$ ceramic capacitor films as reported by Tsai and Tseng [12] and agrees well with those described by Jonscher [25] and Nicollian and Brews [27].

The frequency-dependent capacitance C_f and resistance R_f, where C_f is parallel with R_f can be determined as

follows [28]:

$$G_p(\omega) = a\omega^n = 1/R_f \quad (10)$$

$$B_p(\omega) = b\omega^n = \omega C_f \quad (11)$$

where n is a constant and a and b are coefficients as functions of temperature. Thus, by considering an exponential distribution of admittance and impedance, one can transform the total impedance into an equivalent circuit consisting of a frequency-dependent capacitor, C_f, in parallel with a frequency-dependent resistor, R_f (figure 5). The value of the exponent, n can be determined from the depression angle, θ which is suggested to be associated with the loss degree of the material [28].

The conductance G_p of the Schottky junction at the electrode/film interface can be described as a sum of the shallow trap conductance G_{ts}, the deep trap conductance G_{td} (due to the grain boundary and interface defects) and dc component G_{DC} [9, 12]

$$G_p(\omega, T) = G_{dc} + G_{td}(\omega) + G_{ts}(\omega, T). \quad (12)$$

By applying a small ac signal and varying the temperature, the peak of $G_p(\omega)/\omega$ against ω occurs when the angular frequency of the ac signal equals the emission rate e_n of electrons in a trapping state. Under the ac stress, the intersection of the Fermi energy, E_f, and the shallow trap energy, E_t, varies about its equilibrium position. Therefore, the time dependence of the ensuing charge transition can be expressed as

$$\tau^{-1} = \omega_{re} = e_n = \sigma_n v_{th} N_c \exp[(E_c - E_t)/kT] \quad (13)$$

where ω_{re} is the peak frequency, τ^{-1} is the relaxation time, E_c is the energy of the bottom of the conduction band, k is Boltzmann's constant, σ_n is the capture cross section of the trap, v_{th} is the free electron thermal velocity and N_c is the conduction-band density of states. Figure 6 shows the plot of $G(\omega)/\omega$ against ω of Ta_2O_5 thin films measured at various temperatures. The peak frequency (ω_{re}) shifts to higher temperatures with increasing measurement temperatures. Using equation (13), the trap energy E_t, can be determined by plotting $\ln(\omega_{re})$ against $1000/T$ (figure 7). The plot shows a straight line by the least-squares fit, the slope of which corresponds to the trap energy (E_t), i.e. the trap depth from the bottom of the conduction band. The estimated trap energy (E_t) is around 0.0027 meV, which is much smaller than the thermal energy (kT) 25.9 meV at 27 °C. This indicates that the electrons in the shallow trap states which lie very close to the bottom of the conduction band can acquire sufficient energy, even at room temperature, and exchange between the conduction band and the shallow trap states. In other words, these shallow trap states cannot trap any electrons and undergo exchange of free electrons with the conduction band. Therefore, we envisage that the contribution of shallow defect states on the electrical properties of Ta_2O_5 thin films would be absent for the frequency range of 100 Hz–1 MHz, and hence the proposed equivalent circuit of Ta_2O_5 thin films (figure 5) for the frequency range of 100 Hz–1 MHz do not have the trap level term and it has contributions only from the grain, grain boundary and interface defects.

The capacitance dispersion as a function of frequency from 100 Hz to 1 MHz were used to estimate the defect

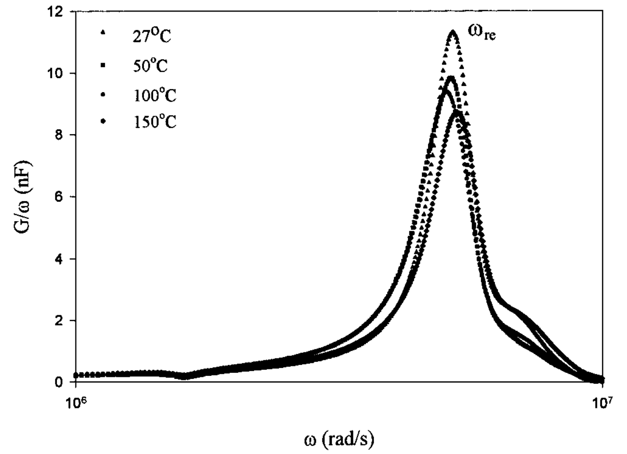

Figure 6. $G(\omega)/\omega$ against ω plot of Ta_2O_5 thin films at various temperatures.

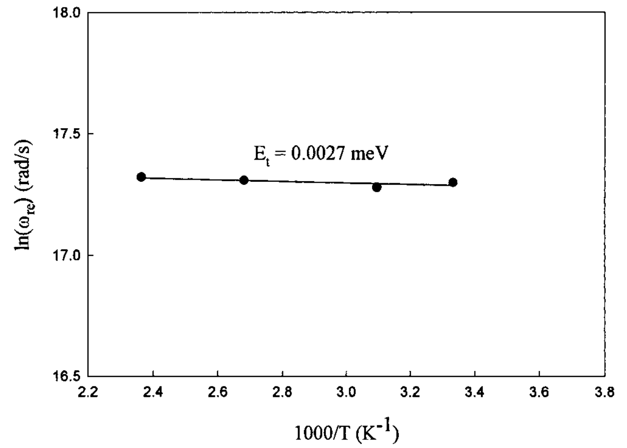

Figure 7. An Arrhenius plot of $\ln(\omega_{re})$ against $1000/T$ of Ta_2O_5 thin films.

density contribution on the relaxation, and hence its influence on the electrical properties. The grain boundary and the interface defects are considered to be donors when the capacitance dispersion becomes neutral or positive by donating an electron. When an ac voltage is applied, the defect levels move up or down with respect to the Fermi level. A change of charge in the defect occurs when it crosses the Fermi level. Therefore, the defect density calculations can be performed from the measurement of the real capacitance (C') and the imaginary part of the capacitance (C'') as a function of frequency. Once C'' is known, the defect density can be obtained from the relation $D_{df} = C''/qA$, where A is the metal plate area and q is the elemental charge [8, 12, 29]. The defect density of the Ta_2O_5 thin film is 8.83×10^{10} cm^{-2} V^{-1}, which is two orders smaller than that observed in perovskite-based dielectric films such as $Ba_{(1-x)}Sr_xTiO_3$ which exhibit significant dielectric relaxation at higher frequencies [12, 30]. Also, the depression angle θ of a semicircular response in the complex impedance (Z) and admittance (Y) planes is non-zero, which corresponds to the distribution of relaxation time as reported [26] and reflects the degree of uniformity in the conductance relaxation. Jonscher [25] showed that θ is related to the extent of the screening effect caused by the hopping charges when it cannot follow the changes of

polarization brought about by an alternating electric field. The θ value of Ta_2O_5 thin film is about 1.3 and is lower that that is observed for $Ba(Sr)TiO_3$ thin films (1.7–2.7) [12] which indicates that Ta_2O_5 thin films exhibit lower screening effects. From the complex capacitance, impedance and admittance studies, we envisage that the dielectric relaxation of Ta_2O_5 films is less pronounced and it has least contribution from the defects, yet preserving a lower leakage current density.

5. Conclusion

In summary, we successfully investigated the dielectric relaxation phenomenon and defect analysis of reactively sputtered Ta_2O_5 thin films, using complex capacitance, impedance and admittance analysis as functions of frequency (100 Hz $\leqslant f \leqslant$ 10 MHz), and temperature (27 °C $\leqslant T \leqslant$ 150 °C). The equivalent circuit proposed here can well explain the ac response of Ta_2O_5 thin films in the frequency range between 100 Hz and 1 MHz, however at frequencies above 1 MHz, the films exhibit resonance in capacitance. The complex admittance measurements proved to be very useful to identify the presence and contribution of defect states on the frequency-dependent resistance, which in turn influences the electrical properties of Ta_2O_5 thin films. On the basis of the complex-plane analysis, we envisage that the effect of shallow defect traps are negligible whereas the grain boundary and interface defects provide significant contribution for the origin of dielectric relaxation. Present studies also demonstrate that dielectric relaxation of Ta_2O_5 films is less pronounced compared to the other dielectric films.

Acknowledgment

The authors gratefully appreciate the financial support from the National Science Council of Republic of China, under project no NSC 87-2218-E 009-008.

References

[1] Zaima S, Furuta T, Yasuda Y and Iida M 1990 *J. Electrochem. Soc.* **137** 1297

[2] Hitchens W R, Krusell W C and Dobkin D B 1993 *J. Electrochem. Soc.* **140** 2615

[3] Saitoh M, Mori T and Tamura H 1996 *IEDM Tech. Dig.* 680

[4] Ezhilvalavan S and Tseng T Y 1999 *J. Mater. Sci.* **10** 9

[5] Kamiyama S, Saeki T, Mori H and Numasawa Y 1991 *IEDM Tech. Digest* 827

[6] Lo G, Kwong D L, Fazan P C, Mathews V K and Sandler N P 1993 *IEEE Electron Devices Lett.* **14** 216

[7] Ezhilvalavan S and Tseng T Y 1999 *J. Am. Ceram. Soc.* **82** 600

[8] Ezhilvalavan S and Tseng T Y 1999 *Appl. Phys. Lett.* **74** 2477

[9] Ezhilvalavan S and Tseng T Y 1998 *J. Appl. Phys.* **83** 4797

[10] Fukuda Y, Aoki K, Numata K and Nishimura A 1994 *Japan. J. Appl. Phys.* **33** 5255

[11] Chen X, Kingon A I, Al-Shareef H N, Bellur K R, Gifford K D and Auciello O 1995 *Integr. Ferroelectr.* **7** 291

[12] Tsai M S and Tseng T Y 1998 *Mater. Chem. Phys.* **57** 47

[13] Kingon A I, Streiffer S K, Basceri C and Summerfelt S R 1996 *Mater. Res. Bull.* **7** 46

[14] Waser R 1995 *Science and Technology of Electroceramic Thin Films (NATO ASI series, vol 284)* ed O Auciello and R Waser (Dordrecht: Kluwer) p 223

[15] Horikawa T, Makita T, Kuroiwa T and Mikami N 1996 *Japan. J. Appl. Phys.* **34** 5478

[16] Alim M A, Seitz M A and Hirthe R W 1988 *J. Appl. Phys.* **63** 2337

[17] Lai C H and Tseng T Y 1994 *IEEE Trans. Comp. Packag. Manufact. Technol.* **17** 309

[18] Watanabe K, Tressler J, Sadamoto M, Lsobe C and Tanaka M 1996 *J. Electrochem. Soc.* **143** 3008

[19] Takemura K, Yamamichi S, Lesaicherre P Y, Tokashiki K, Miyamoto H, Ono H, Miyasaka Y and Yoshida M 1995 *Japan. J. Appl. Phys.* **34** 5224

[20] Waser R, Baiatu T and Hardtl K H 1990 *J. Am. Ceram. Soc.* **73** 1645

[21] Ezhilvalavan S and Kutty T R N 1996 *Appl. Phys. Lett.* **69** 3540

[22] Pike G E 1982 *Mater. Res. Soc. Proc.* **5** 369

[23] Tomozane M, Nannichi Y, Onodera I, Fukase T and Hasegawa F 1988 *Japan. J. Appl. Phys.* **27** 260

[24] Yoon S G and Safari A 1995 *Thin Solid Films* **254** 211

[25] Jonscher A K 1983 *Dielectric Relaxation in Solids* (ISBN 0 9508711 0 9) (London: Chelsa Dielectrics) p 80

[26] Cole K S and Cole R H 1941 *J. Chem. Phys.* **9** 314

[27] Nicollian E H and Brews J R 1982 *MOS (Metal Oxide Semiconductors) Physics and Technology* (New York: Wiley)

[28] McCann J F and Badwal S P S 1982 *J. Electrochem. Soc.* **129** 551

[29] Sze S M 1981 *Physics of Semiconductors* 2nd edn (New York: Wiley) p 380

[30] Tseng T Y 2000 *Ferroelectrics* at press